

Virtual Screening of Natural Compounds Against Six Protein Receptors Coded by The SARS-CoV-2 Genome

Fikry Awaluddin¹, Irmanida Batubara^{1,2*}, Setyanto Tri Wahyudi^{2,3}

¹Department of Chemistry, Faculty of Mathematics and Natural Sciences, IPB University, Bogor 16680, Indonesia;

²Tropical Biopharmaca Research Center, IPB University, Bogor 16128, Indonesia;

³Department of Physics, Faculty of Mathematics and Natural Sciences, IPB University, Bogor 16680, Indonesia

*Corresponding author email: ime@apps.ipb.ac.id

Received July 18, 2021; Accepted February 12, 2023; Available online March 20, 2023

ABSTRACT. Severe Acute Respiratory Syndrome Coronavirus 2 (SARS-CoV-2) is the virus that causes Coronavirus 2019 (COVID-19). To date, there has been no proven effective drug for the treatment or prevention of COVID-19. A study on developing inhibitors for this virus is carried out using molecular docking simulation methods. 3CL-Pro, PL-Pro, Helicase, N, E, and M protein were used as protein targets. Autodock Vina, Autodock 4.2, and PSOVina were used in this study. This study aims to obtain a model of ligands interactions of active natural compounds against the receptor protein encoded by the SARS-CoV-2 genome and their free binding energy to propose active compounds from natural products that have potential as a drug for COVID-19. Corilagin (-14,42 kcal/mol), Scutellarein 7-rutinoside (-13,2 kcal/mol), Genistein 7-O-glucuronide (-10,52 kcal/mol), Biflavonoid-flavone base + 3O (-11,88 and -9,61 kcal/mol), and Enoxolone (-6,96 kcal/mol) has the best free energy value at each protein target indicating that the compound has the potential as a viral protein inhibitor for further investigation. This research is limited to computer simulations, where the results obtained are still a prediction.

Keywords: COVID-19, Molecular Docking, Natural Compound, Sars-CoV-2, Virtual Screening

INTRODUCTION

Severe acute respiratory syndrome coronavirus 2 (SARS-CoV-2), a virus from Coronavirus disease 2019 (COVID-19), has become the center of global attention in 2020. This virus spreads very fast almost all over the world. To date, no drugs and vaccines for the treatment or prevention of COVID-19 have been proven effective. Current treatment focuses only on symptoms (CDC, 2020; FDA, 2020; WHO, 2020).

SARS-CoV-2 is a type of β -coronavirus with a diameter of 60-100 nm and round or oval. SARS-CoV-2 has four important structural protein parts, namely the spike protein (S), envelope (E), membrane (M), and nucleocapsid (N) (Guo et al., 2020). S glycoprotein on the virus's surface can attach and enter into target cells via ACE2 receptors, expressed by epithelial cells of the lungs, intestines, kidneys, and blood vessels. After that, the viral RNA genome is released into the cytoplasm. With the help of ribosomes, the RNA translates polyproteins, namely ppla and pplab, and nonstructural proteins. The polyproteins are broken down into viral protein components by viral proteases, namely Papain-like proteinase (PL-Pro) and Chymotrypsin-like proteinase (3CL-Pro). Subsequently, a replication-transcription complex (RTC) is formed in the multiple membrane vesicles.

RTC continuously replicates and synthesizes the subgenomic RNA bundle encoding proteins. Mediated by the endoplasmic reticulum (ER) and Golgi bodies, new genomic RNA is formed. S, M, E, and N proteins gather to form compartments between the RE-Golgi (ERGIC), becoming virions in the vesicles. Then, the vesicles containing these virions penetrate the plasma membrane to release new viruses (Guo et al., 2020; Li et al., 2020; Maier et al., 2015).

In this mechanism, several essential proteins play a role in virus development. An understanding of the protein found in SARS-CoV-2 is based on various studies reported on SARS-CoV. Understanding the proteins present in these viruses allows for a more rational approach to designing more effective antiviral drugs (Yoshimoto, 2020). PL-Pro and 3CL-Pro are essential for processing the polyproteins that are translated from the viral RNA. Inhibiting the activity of this enzyme would block viral replication. Nucleocapsid protein plays a role in packaging viral RNA into a helical nucleocapsid after being translated and replicated. The Membrane protein is a triple integral membrane protein with a short ectodomain and large carboxyl-terminus endo-domain. Envelope protein has been shown to play a significant role in the assembly of the virus. Another essential protein for

viral replication is Helicase. Recombinant Helicase has multiple enzymatic activities. Inhibiting this protein activity can also prevent replication in viral RNA (Tan et al., 2005). Based on this report, the six proteins explained are the target proteins in this research.

Bioactive compounds from natural products can be an alternative in developing antiviral drugs, including the COVID-19 drug (Kapoor et al., 2017; Lin et al., 2014). It has been reported that some herbal extracts can inhibit viral development in vitro. Herbal extracts from *Cimicifuga rhizoma*, *Coptidis rhizoma*, *Phellodendron cortex*, and *Meliae cortex* can inhibit viral replication in cell culture. Emodin in the genus *Rheum* and *Polygonum* is reported to inhibit the S protein binding of SARS-CoV at the ACE2 receptor. *Artemisia annua*, *Lycoris radiata*, *Lindera aggregata*, *lycorine*, and *Pyrrosia lingua* also showed activity against SARS-CoV. Saikosaponin B2, which is a triterpene glycoside, can inhibit viral adhesion and penetration into host cells. Myricetin and scutellarein act as helicase inhibitors of SARS-CoV. The polyphenolic compound Theaflavin-3,3-digallate (TF3) exhibits antiviral activity by targeting the 3CL-Pro SARS-CoV protein. *Eupatorium fortune* can inhibit the replication of viral RNAs, including SARS-CoV in humans (Culp, 2020).

As a first step in screening active compounds from natural substances that have the potential to have activity against SARS-CoV-2, a study on the development of inhibitors for this virus can be carried out using a molecular docking simulation method. With this method, virtual screening of data sets of active natural compounds that have biological activity can be carried out quickly, effectively, and efficiently. Previous research had been reported that the binding energy value from the docking of 3CL-Pro with ligands of chloroquine and hydroxychloroquine were -7.1 and -6.8 kcal/mol, respectively (Narkhede et al., 2020). Other docking study indicated that kaempferol (-8.58 kcal/mol), quercetin (-8.47 kcal/mol), luteolin-7glucoside (-8.17 kcal/mol), demethoxycurcumin (-7.99 kcal/mol), naringenin (-7.89 kcal/mol), apigenin-7-glucoside (-7.83 kcal/mol), oleuropein (-7.31 kcal/mol), curcumin (-7.05 kcal/mol), catechin (-7.24 kcal/mol), and epicatechin-gallate (-6.67 kcal/mol) have the potential to act as COVID-19 M^{Pro} Inhibitor (Khaerunnisa et al., 2020). This research will carry out the docking of molecules of active natural compounds to several receptor proteins coded by the SARS-CoV-2 genome as a series of searches for COVID-19 drug candidates. Autodock Vina, Autodock 4.2, and PSOVina were used in this study. This study aims to obtain a model of the ligand molecular binding interaction of bioactive natural compounds against the receptor protein encoded by the SARS-CoV-2 genome and its free binding energy to propose bioactive compounds that have potential as COVID-19 drugs for further research.

EXPERIMENTAL SECTION

Hardware Specifications

The hardware used in this research is a computer with Intel® Core™ i3, 16 GB RAM, and 4 GB NVIDIA Optimus Ge Force GTX 970 Graphic Card, with the Windows 10 Pro 64 bit Operating system.

Preparation of The Three-Dimensional Structure of The Protein

The three-dimensional structure of proteins used in this study were six receptor proteins encoded by the SARS-CoV-2 genome, namely 3CL-Pro (PDB ID: 6WNP), PL-Pro (PDB ID: 6WX4), Helicase (PDB ID: 6JYT), Nucleocapsid (PDB ID: 6VYO), and Envelope (PDB ID: 6VYO) protein obtained from a protein data bank (<http://www.rcsb.org/pdb/>) and the Membrane protein (QHD43419) obtained from I-Tasser products produced by Zhang Laboratory, University of Michigan (Zhang et al., 2020). Protein macromolecules are separated from solvents and ligands or nonstandard residue. The separation of macromolecules from unnecessary molecules and optimization of molecules was carried out using the Autodock Tools program. Then, the optimization is done by adding polar hydrogen atoms and setting the grid box parameter. The grid box set uses the Autoligand feature (Harris et al., 2008) in Autodock to determine the ligand-binding site's position according to the lowest energy obtained from the scan. These results are saved in pdbqt format. The protein binding site was visualized with VMD molecular graphics software (Humphrey et al., 1996).

Ligand Preparation

The ligands used are 1113 compounds that include natural compounds and their analogs reported as antivirals from various published literature in scientific journals from 2012 to 2020. The literature search uses a search engine with the keyword "Antiviral natural compound and antiviral herbal." As a comparison, vitamins and drugs that have been used as therapy for COVID-19 are also used (Culp, 2020). The structures were obtained from PubChem (<http://PubChem.ncbi.nlm.nih.gov>) in sdf format. The format of these ligands was converted to pdb using Open Babel (Hutchinson et al., 2020). The ligand structure that has been made was optimized with Autodock Tools. These results were saved in the pdbqt format (Morris et al., 2010).

Virtual Screening

Autodock vina (Trott & Olson, 2009) is used for virtual screening of the ligand database against six target proteins prepared and optimized beforehand with Autodock Tools. At this stage, the free binding energy value of Gibbs (ΔG) from each ligand to the target protein is obtained. Then the ligand with the lowest energy value is selected to be processed to the next stage.

Molecular Docking

The best ligands obtained from the virtual screening were redocked with Autodock 4.2. In this study, the Lamarckian Genetic Algorithm (LGA) was used as a scoring function. The five ligands with the lowest free binding energy were selected to be redocked with 1000 iterations using PSOVina (Ng et al., 2015). Each value obtained from the docking process was calculated as the average value to get the three ligands with the best results.

Analysis of Protein-Ligand Interactions

The result of protein-ligand docking was visualized by Biovia Discovery Studio. The protein and ligand interactions were analyzed by observing the hydrogen bonds and hydrophobic interactions.

RESULT AND DISCUSSION

Determination of Target Protein Binding Sites

Autoligand scanning was carried out with three fill points with 100, 200, and 300. The energy value was obtained from each fill point, then the lowest value of each protein was selected, which was used as a reference in determining the ligand-binding site (Figure 1). The 3CL-Pro protein produced -0.17669923 kcal/mol total energy per volume for 302 Å³. Volume represents the binding site area, while the total energy per volume means the binding energy produced at the scanned volume. PL-Pro showed a lower value than 3CL-Pro, which is -0.19145122 kcal/mol and a total volume of 311 Å³. Helicase at volume 282 Å³ exhibited the lowest binding energy compared to other proteins at -0.21382078 kcal/mol. The nucleocapsid protein showed -0.1795932 kcal/mol and 318 Å³. The envelope protein presented

values of -0.12641521 kcal/mol and 305 Å³. The Membrane protein exhibited a value of -0.17621889 kcal/mol at a volume of 323 Å³. From these results, the grid box parameters were determined according to Table 1.

Virtual screening

Based on the virtual screening result of 1113 ligands docked to the six target proteins, the Gibbs free binding energy (ΔG) data obtained from each of these ligands. The ligands with the best rank with the lower energy value among all ligands were selected for further processing with Autodock 4.2. At this stage, 82 ligands with the lowest free energy values on each protein were determined. On the other hand, drugs of lopinavir and nafamostat were selected as positive controls (Table 2). The positive controls were selected based on virtual screening results with the best free binding energy for each target protein.

Virtual screening is a method for selecting compounds that have potential activity from a database of chemical compounds. These compounds are docked to the target protein binding site, resulting in a ranking of the compounds based on the protein-ligand complexes' binding affinity. Because this virtual screening involves 1113 compounds, this stage was carried out to determine which compound will be selected based on the best ranking as a potential compound to proceed to the next stage (Ferreira et al., 2015). Autodock Vina was used for virtual screening because of its more straightforward scoring function, which allows for faster search methods and reproduces larger systems with 20 flexible bonds (Morris et al., 2010).

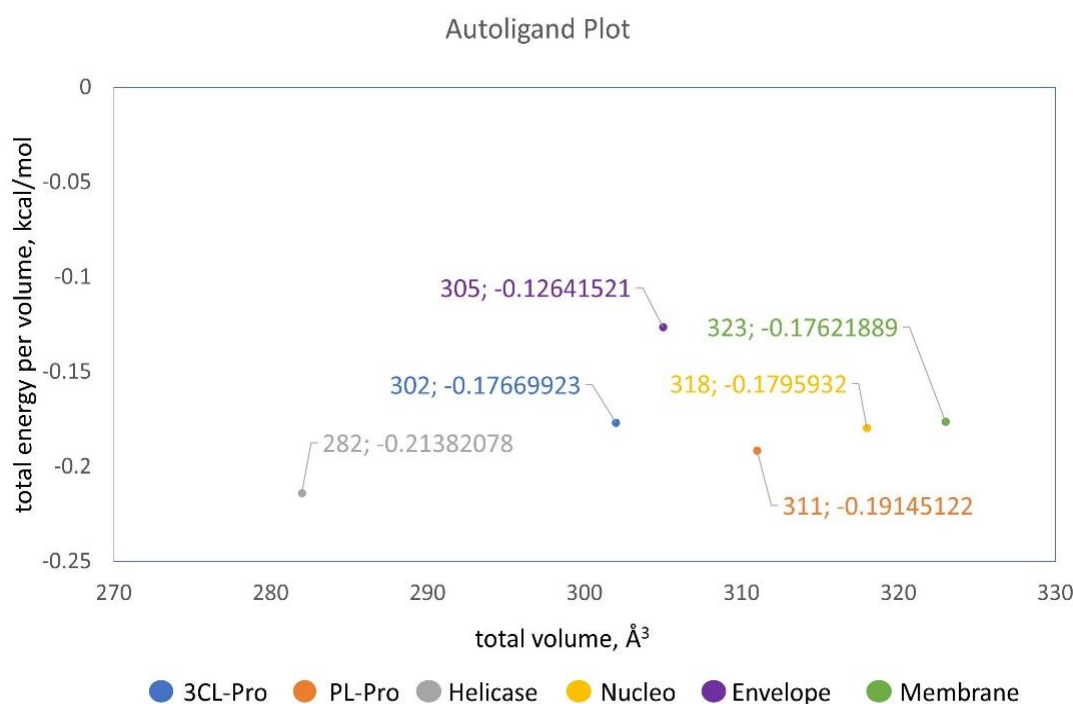


Figure 1. The lowest free energy binding site of six proteins

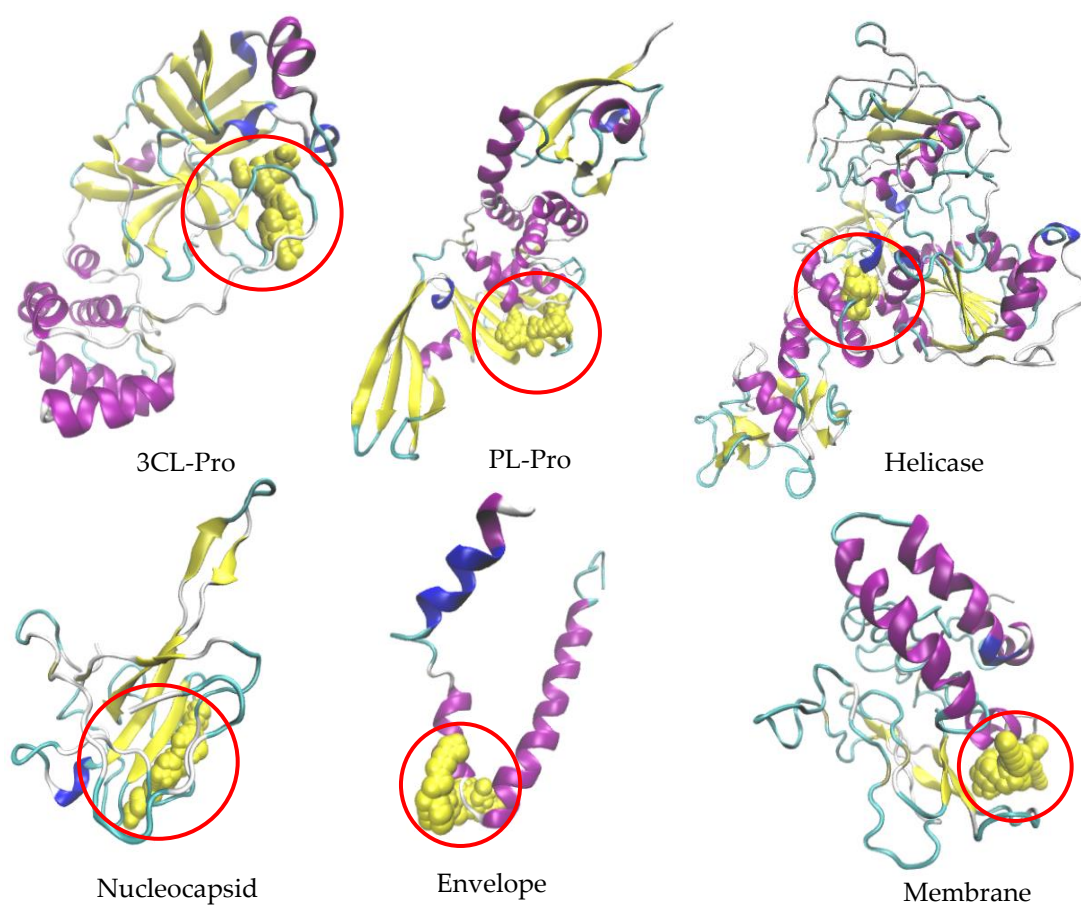
Table 1. Grid box parameters of the six protein for molecular docking

Protein	Code ID	center_x	center_y	center_z	size_x	size_y	size_z
3CL-Pro	6WNP	6,954	25,881	23,585	20	20	20
PL-Pro	6WX4	8,592	-24,397	-36,705	24	24	24
Helicase	6JYT	422,998	25,254	72,826	20	18	18
Nucleocapsid	6VYO	-17,943	-7,41	-9,968	20	24	20
E-Channel	5X29	3,001	-15,638	17,255	20	20	20
Membrane	QHD43419	70,994	56,082	53,99	20	28	25

num_modes = 3

exhaustiveness = 8

spacing = 1 Å

**Figure 2.** Binding site of each target protein (yellow marked with a red circle).**Table 2.** Selected ligands resulting from virtual screening

No.	Ligand	Protein Target
1	Galloyl quercitrin	3CL-Pro
2	Sanggenol O	
3	Corilagin	
4	Epoxy-tannin	
5	Sanggenol N	
6	Dihydro-tannin	
7	Cyanidin 3-O-rutinoside betaine	
8	d-Berberamine	
9	Proanthocyanidin A1	

10	Procyanidin B5	
11	Withaferin A	
12	Lopinavir	
13	Tellimagrandin II	
14	9-O-(Piperonyl) berberrubine chloride	
15	Narasin A	
16	Sanggenol H	
17	Cepharanthine	
18	Inophyllum D	PL-Pro
19	Inophyllum P	
20	Quercetin 4'-glucuronide	
21	Withanolide F	
22	(E)-1-(2-Hydroxy-4-methoxyphenyl)-3-[3-[(E)-3-(2-hydroxy-4-methoxyphenyl)-3-oxoprop-1-enyl]phenyl]prop-2-en-1-one	
23	Folic Acid (Vit. B9)	
24	Dehydropipernonaline	
25	Catechin 7-O-gallate	
26	3,5-Dicaffeoylquinic acid	
27	Acanthoside C	
28	Genistein 7-O-glucuronide	
29	Pipernonaline	Helicase
30	Ruberythric acid	
31	1,5-Dicaffeoylquinic acid	
32	Genistein 7-glucoside	
33	Methyl 3,5-di-O-caffeoyl quinate	
34	Genistoside	
35	Neochlorogenic acid	
36	1,3-Dicaffeoylquinic acid	
37	Hesperetin-7-rutinoside	
38	Naringenin-7-O-rutinoside	
39	Samarangenin	
40	Isotheaflavin-3-gallate	
41	Alpha-Glycyrrhizin	Protein N
42	Withanolide O	
43	Eleutheroside I / Mubenin B	
44	Digitoxin	
45	Digoxin	
46	Vincetoxicoside B	
47	Aurantiamide acetate	
48	(+)-Balsacone L	
49	N-benzyl brucine	
50	Sanggenol L	
51	Withanolide L	
52	Balsacone P	Protein E
53	(-)-Balsacone J	
54	(-)-Balsacone L	
55	Oleanol	
56	Oleanane	
57	Enoxolone	
58	Proanthocyanidin B2	
59	Withanolide A	Protein M
60	Genkwanol B	
61	Procyanidin B3	

62	Stelleranol	
63	Procyanidin B1	
64	Sanggenol J	
65	Ginkgetin	
66	Bilobetin	
67	Sciadopitysin	
68	Hypericin	
69	Glycyrrhizin	3CL-Pro; Protein N
70	Theaflavin-3,3-digallate	
71	Amentoflavone	3CL-Pro; PI-Pro; Protein M
72	Biflavonoid-flavone base + 3O	3CL-Pro; PI-Pro; Protein N; Protein M
73	Cyanidin 3-O-(6-O-p-coumaroyl)glucoside	
74	Scutellarein 7-rutinoside	PL-Pro; Protein N
75	Biflavonoid-flavone base + 3O and flavone base + 3O + 1Prenyl	PL-Pro; Protein M
76	Swerilactone K	
77	(-)-Balsacone K	
78	Withanolide	Protein N; Protein E
79	Withanolide B	
80	Digitoxin acetone	Protein E; Protein M
81	Amentoflavone dimethyl ether	PL-Pro; Protein N; Protein M
82	Nafamostat	PI-Pro; Helicase; Protein N; Protein E; Protein M

Molecular Docking

The results of Autodock 4.2 showed that the value of the binding energy (ΔG) varies (**Table 3**). When compared with the positive control, several compounds had better binding energy values. Five ligands with the best value were selected from each target protein to be compared with the positive control. Free binding energy data from Autodock 4.2 can be seen in **Table 3**. Corilagin produced the best free binding energy value (-14.42 kcal/mol) than other ligands and positive control on docking to 3CL-Pro. Scutellarein 7-rutinoside (-13,2 kcal/mol) produced the lowest energy value on docking to PL-Pro. Genistein 7-O-glucuronide (-10,52 kcal/mol) exhibited the lowest energy values on docking to Helicase. Biflavonoid-flavone base + 3O produced the best value on the two proteins docked to it, nucleocapsid (-11,88 kcal/mol) and membrane (-9,61 kcal/mol) protein. On docking with envelope proteins, Enoxolone (-6,96 kcal/mol) showed the lowest energy value.

In the next step, the selected ligands were redocked using PSOVina. In **Figure 3**, it can be seen that all the tested ligands produced a consistent graph to determine the best ligand based on the average value of its free binding energy on 1000 repetitions of molecular docking (**Table 3**). At this stage, Sanggenol O (-9.38 kcal/mol) produced the lowest energy value better than corilagin for 3CL-Pro protein. Swerilactone K (-8.25 kcal/mol) docked to PL-Pro showed the lowest energy value. In Helicase protein, Genistein 7-O-glucuronide (-8.71 kcal/mol) produced the lowest

energy. Hypericin (-8.50 kcal/mol) has the lowest energy in docking to Nucleocapsid protein. Enoxolone (-6.39 kcal/mol) docked to Envelope protein has the lowest energy. Biflavonoid-flavone base + 3O (-8.33 kcal/mol) presented the lowest binding energy for docking to a Membrane protein.

Compared with the best energy value of Autodock 4.2 results, Corilagin in 3CL-Pro, Scutellarein 7-rutinoside in PL-Pro, and Biflavonoid-flavone base + 3O in nucleocapsid protein had good docking consistency. However, the average energy values obtained were not the best. While Genistein 7-O-glucuronide in Helicase, Enoxolone in Envelope protein, and Biflavonoid-flavone base + 3O in Membrane protein produced the best average energy value.

During the virtual screening, Autodock Vina ignores the charge present on the protein and ligand molecules. Using Autodock 4.2, minimizing ligand energy can affect the docking results, which helps ensure that bond regularity, bond length, and bond angle are correct (Schulig & J Richardson, 2020). The ligands with the best energy values obtained from the screening results were processed with Autodock 4.2 docked to each target protein.

PSOVina uses a particle swarm optimization (PSO) algorithm with the efficient Broyden-Fletcher-Goldfarb-Shannon (BFGS) local search method adopted in AutoDock Vina to solve the problem of finding conformations in docking. PSOVina cut execution time by 51-60% without compromising docking accuracy (Ng et al., 2015).

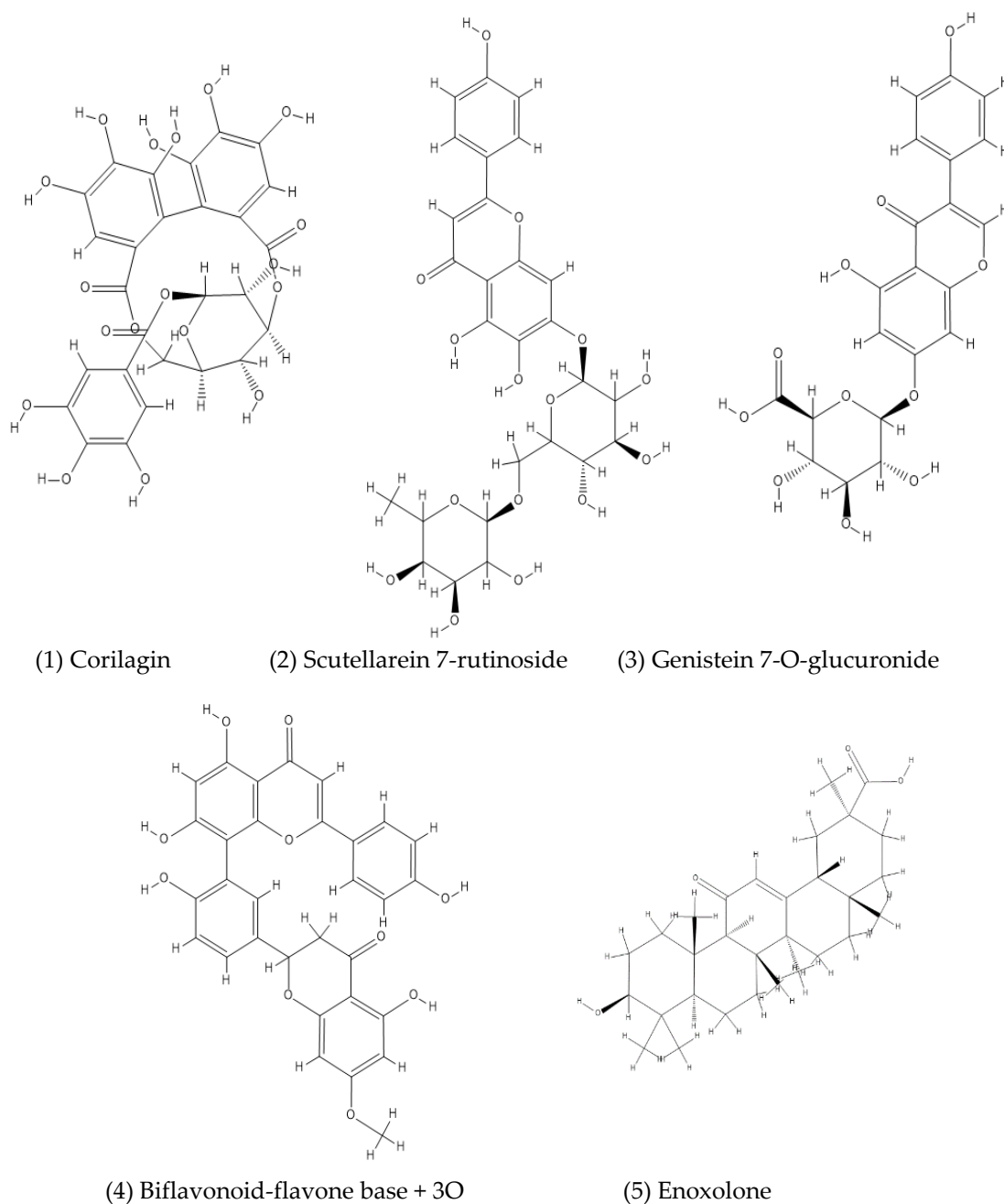


Figure 3. Structures of the selected ligands

Table 3. The binding energy of the ligands at each receptor

PROTEIN TARGET	LIGANDS	AUTODOCK 4.2 ΔG (kcal/mol)	PSOVINA ΔG (kcal/mol)
3CL-PRO	Corilagin	-14.42	-8.00
	Sanggenol N	-11.12	-7.72
	Galloyl quercitrin	-10.6	-7.81
	Sanggenol O	-10.31	-9.38
	Withaferin A	-10.21	-7.29
	Lopinavir	-11.52	-
PL-PRO	Scutellarein 7-rutinoside	-13.2	-6.90
	Biflavonoid-flavone base + 3O	-9.48	-7.61
	Swerilactone K	-9.38	-8.25
	Amentoflavone	-9.22	-8.05

	Biflavonoid-flavone base + 3O and Flavone base + 3O + 1Prenyl	-9.13	-7.89
	Nafamostat	-12.55	-
HELICASE	Genistein 7-O-glucuronide	-10.52	-8.71
	Piperonaline	-9.42	-7.55
	Dehydropiperonaline	-9.39	-7.58
	Genistoside	-9.38	-7.85
	Genistein 7-glucoside	-9.26	-8.25
	Nafamostat	-8.94	-
NUCLEOCAPSID	Biflavonoid-flavone base + 3O	-11.88	-7.94
	Amentoflavone dimethyl ether	-11.25	-7.21
	Isotheaflavin-3-gallate	-11.01	-6.83
	Hypericin	-10.57	-8.50
	(-)-Balsacone K	-10.49	-6.56
	Nafamostat	-9.72	-
ENVELOPE	Enoxolone	-6.96	-6.39
	Oleanane	-6.5	-5.75
	Oleanol	-6.06	-5.71
	Withanolide B	-6.05	-5.44
	Withanolide	-6.03	-5.42
	Nafamostat	-5.17	-
MEMBRANE	Biflavonoid-flavone base + 3O	-9.61	-8.33
	Digitoxin acetone	-9.57	-5.72
	Withanolide A	-9.3	-8.14
	Withanolide B	-9.29	-7.60
	Sciadopitysin	-9.24	-8.19
	Nafamostat	-7.65	-

Protein-Ligand Interaction

Ligands with the six proteins' lowest energy values, hydrogen bonding, and hydrophobic interactions were observed (Figure 5). Corilagin formed hydrogen bonds with six residues Gln192, Glu166, His41, His164, Gln189, and Asn142, then three hydrophobic interactions Ala191, Pro168, and Met165, and showed pi-sulfur interaction via Cys145 in docking to 3CL-Pro.

Scutellarein 7-rutinoside that docked to PL-Pro showed four hydrogen bonds with residues Tyr264, Gly266, Tyr273, and Gly271, as well as two pi-alkyl interactions formed with Tyr268 and Leu162. In Helicase, Genistein 7-O-glucuronide presented seven hydrogen bonds with Tyr120, Tyr382, Asp383, Lys139, Glu142, and Arg409, while Thr380 formed pi-donor hydrogen bond. Three other residues were Leu138, Ala135, and Ala123 showed hydrophobic interactions.

Biflavonoid-flavone base + 3O produced the best energy value in two proteins, nucleocapsid and membrane protein types. This ligand showed eight hydrogen bonds Lys127, Ala125, Phe66, Gln70, Ala134, Gly69, Trp132, Asn126, and four hydrophobic interactions Ala134, Val133, Tyr123, and Arg68, while Ile130 showed pi-lone pair interaction when docked to nucleocapsid. The membrane proteins showed four hydrogen bonds via

Tyr196, Arg72, Thr77 and Ala183, and six hydrophobic interactions with residues of Leu138, Ala195, Val139 (alkyl interaction), Asn74, Trp75 (pi-pi interaction), and Ala81 (alkyl interaction).

Enoxolone has three hydrogen bonds Thr35, Ala40, and Leu39 docked to envelope proteins. Moreover, for hydrophobic interactions, it interacted with Arg38, Ala41 and Tyr42 residues.

Herbal Source of The Selected Ligands

Corilagin is an ellagitannin compound found in *Phyllanthus* species such as *Phyllanthus amarus*, *P. emblica*, *P. niruri*, *P. urinaria*, *P. reticulatus*, *P. virgatus*. This species is distributed over most of the tropics and subtropics, including Africa, America, Oceania, and Asia (Jantan et al., 2019). In Indonesia, *P. niruri* known as Meniran Hijau, has been empirically used by Indonesians as a traditional medicine for pain relief (Sutrisna et al., 2019). Some reports indicated the antiviral activity of corilagin. Reddy et al. reported that Corilagin from *P. amarus* inhibits the key Hepatitis C Virus (HCV) enzymes, NS3 protease, and NS5B RdRp in vitro and inhibits HCV replication in the infectious cell culture system (Reddy et al., 2018). Corilagin also has an antiviral effect on Human enterovirus 71 (EV71) and Coxsackievirus A16 (CA16) in vitro (Yeo et al., 2015). It could reduce Human Immunodeficiency Virus (HIV) replication by inhibiting the HIV-1 protease and HIV-1 integrase enzymes (Notka et al., 2004).



Figure 4. Graphs of PSO Vina redocking results with 1000 iterations for each protein

Scutellarein 7-rutinoside belongs to the flavonoid group contained in the *Oroxylum indicum* (Linn) Vent. *O. indicum* is commonly known as Sonaphata, Sona, Shyonaaka, and Indian trumpet tree. It grows in India and is used as traditional Ayurveda medicine (Bhardwaj, 2018). Scutellarein 7-rutinoside is a derivative of scutellarein, which is found in *Scutellaria baicalensis*. This plant has been widely used in traditional Chinese medicine to treat viral infection-related symptoms. Scutellarein in *S. baicalensis* was reported to inhibit the SARS-CoV-2 3CL-Pro in vitro (Liu et al., 2020). Scutellarein was reported could inhibit the SARS-CoV protein helicase in vitro by affecting ATPase activity, but not unwinding activity, nsp13 (Yu et al., 2012). It indicates its potential as an anti-SARS-CoV-2 agent.

Genistein is an isoflavone group contained in soybeans. Genistein 7-O-glucuronide is a glycosylated form of genistein obtained from soybeans

fermentation (Boonpawa et al., 2017). LeCher et al. reported genistein's therapeutic potential as an effective antiviral agent against the Herpes B virus by targeting an event post-viral replication (LeCher et al., 2019). Another study said that genistein could block the viral protein U (Vpu) ion channel in HIV type 1 (Sauter et al., 2014).

Biflavonoid-flavone base+3O is a group of biflavonoids derivatives of amentoflavone with different substitution positions and types in natural plants. Amentoflavone exists in a large number of plants. Some of them have been used as traditional medicines in various countries, such as *Ginkgo biloba*, *Lobelia chinensis*, *Polygala sibirica*, *Ranunculus ternatus*, *Selaginella pulvinata*, *Selaginella tamariscina*, *Calophyllum inophyllum*, *Selaginella bryopteris*, *Byrsonima intermedia*, *Cnestis ferruginea*, and *Drypetes gerrardii*. Amentoflavone exhibited its anti-dengue potential by inhibiting Dengue virus NS5

RdRp. Amentoflavone was proved as the most active one to inhibit SARS-CoV concluded relative to the inhibition of 3CL-Pro. Amentoflavone was also found to decrease Coxsackievirus B3 (CVB3) replication by inhibiting fatty acid synthase expression. Moreover, in HIV and respiratory syncytial virus (RSV) cases, amentoflavone showed good activity (Yu et al., 2017).

Enoxolone or glycyrrhetic acid is a pentacyclic triterpenoid aglycone metabolite of glycyrrhizin produced by *Glycyrrhiza glabra* (licorice). This species

is a native of Mediterranean areas and Asia, especially the central and south-western parts. The root of this plant is widely used for treating upper respiratory tract and gastric ulcer diseases. Antiviral activity of glycyrrhizin and its derivatives revealed in vivo or in vitro against hepatitis B and C viruses, herpes simplex virus, influenza A, HIV-1, EV71, SARS-related coronavirus, RSV, vesicular stomatitis virus, vaccinia virus, and arboviruses (Langer et al., 2016).

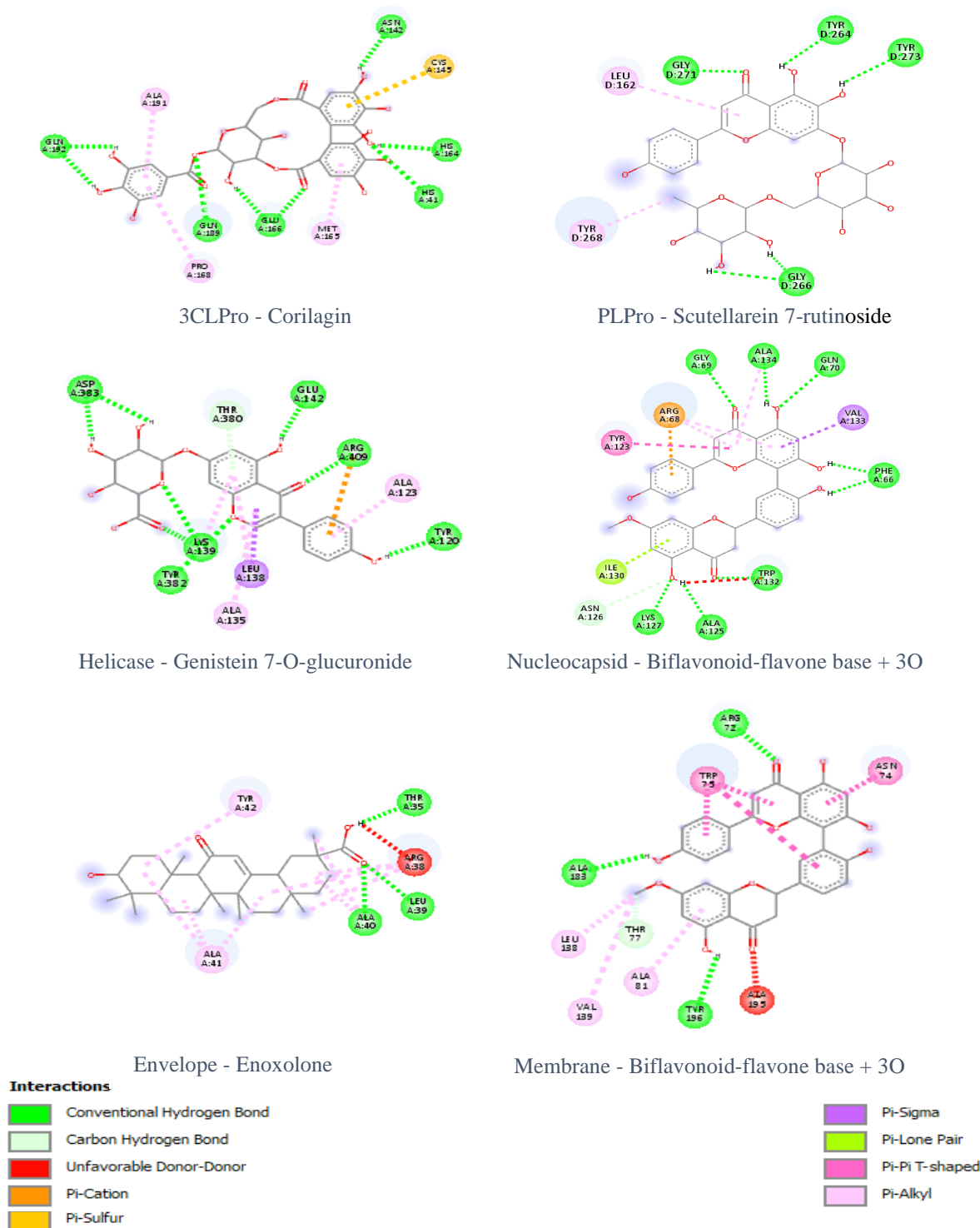


Figure 5. Interaction of ligands with amino acid residues on target protein

CONCLUSIONS

Several bioactive compounds with potential inhibitors against six receptor proteins encoded by the Sars-CoV-2 genome were obtained through virtual screening and molecular docking. Corilagin (-14.42 kcal/mol), Scutellarein 7-rutinoside (-13,2 kcal/mol), Genistein 7-O-glucuronide (-10,52 kcal/mol), Biflavonoid-flavone base + 3O (-11,88 kcal/mol and -9,61 kcal/mol), and Enoxolone (-6,96 kcal/mol) were compounds that produced the best free energy values on their respective protein targets. These compounds can be further investigated to determine their antiviral activity against Sars-CoV-2 developed as COVID-19 therapy.

ACKNOWLEDGMENTS

The authors would like to thank Indonesia Endowment Fund for Education, Ministry of Finance of the Republic of Indonesia, to fund my studies at the Department of Chemistry, Faculty of Mathematics and Natural Sciences, IPB University, Bogor.

REFERENCES

- Bhardwaj, A. (2018). A Phyto-pharmacological overview on *Oroxylum Indicum* (Linn.) Vent. *International Journal of Advanced Research*, 6(8), 291–297. <https://doi.org/10.21474/IJAR01/7521>
- Boonpawa, R., Spenkelink, A., Punt, A., & Rietjens, I. M. C. M. (2017). In vitro-in silico-based analysis of the dose-dependent in vivo oestrogenicity of the soy phytoestrogen genistein in humans. *British Journal of Pharmacology*, 174(16), 2739–2757. <https://doi.org/10.1111/bph.13900>
- CDC. (2020). Interim clinical guidance for management of patient with confirmed coronavirus disease (COVID-19). Retrieved from centers for disease control and prevention website: <https://www.cdc.gov/coronavirus/2019-ncov/hcp/clinical-guidance-management-patients.html>
- Culp, W. C. (2020). Coronavirus disease 2019 (COVID-19). In S. K. Saxena (Ed.), *A & A Practice*. Singapore: Springer Singapore. <https://doi.org/10.1007/978-981-15-4814-7>
- FDA. (2020). Medical countermeasures. retrieved from food and drug administration website: <https://www.fda.gov/emergency-preparedness-and-response/counterterrorism-and-emerging-threats/coronavirus-disease-2019-covid-19>
- Ferreira, L. G., Dos Santos, R. N., Oliva, G., & Andricopulo, A. D. (2015). Molecular docking and structure-based drug design strategies. In *Molecules*, 20. <https://doi.org/10.3390/molecules200713384>
- Guo, Y. R., Cao, Q. D., Hong, Z. S., Tan, Y. Y., Chen, S. D., Jin, H. J., ... Yan, Y. (2020). The origin, transmission and clinical therapies on coronavirus disease 2019 (COVID-19) outbreak - an update on the status. *Military Medical Research*, 7(1), 11. <https://doi.org/10.1186/s40779-020-00240-0>
- Harris, R., Olson, A. J., & Goodsell, D. S. (2008). Automated prediction of ligand-binding sites in proteins. *Proteins: Structure, Function, and Bioinformatics*, 70(4), 1506–1517. <https://doi.org/10.1002/prot.21645>
- Humphrey, W., Dalke, A., & Schulten, K. (1996). VMD: Visual molecular dynamics. *Journal of Molecular Graphics*, 14(1), 33–38. [https://doi.org/10.1016/0263-7855\(96\)00018-5](https://doi.org/10.1016/0263-7855(96)00018-5)
- Hutchinson, G. R., Swain, C., Morley, C., James, C., Winter, H. De, Vandermeersch, T., & O'Boyle, N. M. (2020). *Open Babel Documentation*.
- Jantan, I., Haque, M. A., Ilangkovan, M., & Arshad, L. (2019). An insight into the modulatory effects and mechanisms of action of phyllanthus species and their bioactive metabolites on the immune system. *Frontiers in Pharmacology*, 10(JULY), 1–19. <https://doi.org/10.3389/fphar.2019.00878>
- Kapoor, R., Sharma, B., & Kanwar, S. S. (2017). Antiviral phytochemicals: An overview. *Biochemistry & Physiology: Open Access*, 06(02). <https://doi.org/10.4172/2168-9652.1000220>
- Khaerunnisa, S.; Kurniawan, H.; Awaluddin, R.; Suhartati, S.; Soetjipto, S. (2020). Potential inhibitor of COVID-19 main protease (Mpro) from several medicinal plant compounds by molecular docking study. *Preprints 2020*, 2020030226 (doi:10.20944/preprints202003.0226.v1).
- Langer, D., Czarzynska-Goslinska, B., & Goslinski, T. (2016). Glycyrrhetic acid and its derivatives in infectious diseases. *Current Issues in Pharmacy and Medical Sciences*, 29(3), 118–123. <https://doi.org/10.1515/cipms-2016-0024>
- LeCher, J. C., Diep, N., Krug, P. W., & Hilliard, J. K. (2019). Genistein has antiviral activity against herpes b virus and acts synergistically with antiviral treatments to reduce effective dose. *Viruses*, 11(6), 499. <https://doi.org/10.3390/v11060499>
- Li, X., Geng, M., Peng, Y., Meng, L., & Lu, S. (2020). Molecular immune pathogenesis and diagnosis of COVID-19. *Journal of Pharmaceutical Analysis*, 19(xxxx), 1–7. <https://doi.org/10.1016/j.jpha.2020.03.001>
- Lin, L. T., Hsu, W. C., & Lin, C. C. (2014). Antiviral natural products and herbal medicines. *Journal of Traditional and Complementary Medicine*, 4(1), 24–35. <https://doi.org/10.4103/2225-4110.124335>
- Liu, H., Ye, F., Sun, Q., Liang, H., Li, C., Lu, R., ... Lai, L. (2020). Scutellaria baicalensis extract and

- baicalein inhibit replication of SARS-CoV-2 and its 3C-like protease in vitro. *BioRxiv*, 2020. 04.10.035824. <https://doi.org/10.1101/2020.04.10.035824>
- Maier, H. J., Bickerton, E., & Britton, P. (2015). Coronaviruses : An overview of their replication and pathogenesis. In H. J. Maier, E. Bickerton, & P. Britton (Eds.), *Coronaviruses: Methods and Protocols*. New York, NY: Springer New York. <https://doi.org/10.1007/978-1-4939-2438-7>
- Morris, G. M., Goodsell, D. S., Pique, M. E., Lindstrom, W., Huey, R., Forli, S., ... Olson, A. J. (2010). AutoDock Version 4.2 - user guide. retrieved from guide website: <http://autodock.scripps.edu/>
- Narkhede RR, Cheke RS, Ambhore JP, Shinde SD. The Molecular docking study of potential drug candidates showing anti-COVID-19 activity by exploring of therapeutic targets of SARS-CoV-2. *EJMO* 2020;4(3):185–195.
- Ng, M. C. K., Fong, S., & Siu, S. W. I. (2015). PSOVina: The hybrid particle swarm optimization algorithm for protein–ligand docking. *Journal of Bioinformatics and Computational Biology*, 13(03), 1541007. <https://doi.org/10.1142/S0219720015410073>
- Notka, F., Meier, G., & Wagner, R. (2004). Concerted inhibitory activities of *Phyllanthus amarus* on HIV replication in vitro and ex vivo. *Antiviral Research*, 64(2), 93–102. <https://doi.org/10.1016/j.antiviral.2004.06.010>
- Reddy, B. U., Mullick, R., Kumar, A., Sharma, G., Bag, P., Roy, C. L., ... Das, S. (2018). A natural small molecule inhibitor corilagin blocks HCV replication and modulates oxidative stress to reduce liver damage. *Antiviral Research*, 150, 47–59. <https://doi.org/10.1016/j.antiviral.2017.12.004>
- Sauter, D., Schwarz, S., Wang, K., Zhang, R., Sun, B., & Schwarz, W. (2014). Genistein as antiviral drug against HIV ion channel. *Planta Medica*, 80(08/09), 682–687. <https://doi.org/10.1055/s-0034-1368583>
- Schulig, L., & J Richardson, R. (2020). What is the major difference/s between Autodock 4.0 and Autodock Vina? Retrieved from Researchgate website: https://www.researchgate.net/post/What_is_the_major_difference_s_between_Autodock_40_and_Autodock_Vina_And_what_is_the_difference_between_adding_charges_by_A_MBER_or_by_Marvin
- Sutrisna, E., Maryati, Wahyuni, S., & S, T. A. (2019). Anti-inflammatory Effect of *Phyllanthus niruri* L. from Indonesia (Pre-clinical Study). *Pharmacognosy Journal*, 11(6).
- Tan, Y. J., Lim, S. G., & Hong, W. (2005). Characterization of viral proteins encoded by the SARS-coronavirus genome. *Antiviral Research*, 65(2), 69–78. <https://doi.org/10.1016/j.antiviral.2004.10.001>
- Trott, O., & Olson, A. J. (2009). AutoDock Vina: Improving the speed and accuracy of docking with a new scoring function, efficient optimization, and multithreading. *Journal of Computational Chemistry*, 31(2), NA-NA. <https://doi.org/10.1002/jcc.21334>
- WHO. (2020). *Clinical management of severe acute respiratory infection when COVID-19 is suspected (v1.2)*. 1–21. Retrieved from [https://www.who.int/publications-detail/clinical-management-of-severe-acute-respiratory-infection-when-novel-coronavirus-\(ncov\)-infection-is-suspected](https://www.who.int/publications-detail/clinical-management-of-severe-acute-respiratory-infection-when-novel-coronavirus-(ncov)-infection-is-suspected)
- Yeo, S.-G., Song, J. H., Hong, E.-H., Lee, B.-R., Kwon, Y. S., Chang, S.-Y., ... Ko, H.-J. (2015). Antiviral effects of *Phyllanthus urinaria* containing corilagin against human enterovirus 71 and Coxsackievirus A16 in vitro. *Archives of Pharmacal Research*, 38(2), 193–202. <https://doi.org/10.1007/s12272-014-0390-9>
- Yoshimoto, F. K. (2020). The Proteins of severe acute respiratory syndrome Coronavirus-2 (SARS CoV-2 or n-COV19), the cause of COVID-19. *Protein Journal*, 39(3), 198–216. <https://doi.org/10.1007/s10930-020-09901-4>
- Yu, M.-S., Lee, J., Lee, J. M., Kim, Y., Chin, Y.-W., Jee, J.-G., ... Jeong, Y.-J. (2012). Identification of myricetin and scutellarein as novel chemical inhibitors of the SARS coronavirus helicase, nsP13. *Bioorganic & Medicinal Chemistry Letters*, 22(12), 4049–4054. <https://doi.org/10.1016/j.bmcl.2012.04.081>
- Yu, S., Yan, H., Zhang, L., Shan, M., Chen, P., Ding, A., & Li, S. (2017). A Review on the phytochemistry, pharmacology, and pharmacokinetics of amentoflavone, a naturally-occurring biflavonoid. *Molecules*, 22(2), 299. <https://doi.org/10.3390/molecules22020299>
- Zhang, C., Zheng, W., Huang, X., Bell, E. W., Zhou, X., & Zhang, Y. (2020). Protein structure and sequence reanalysis of 2019-nCoV genome refutes snakes as its intermediate host and the unique similarity between its spike protein insertions and HIV-1. *Journal of Proteome Research*, 19(4), 1351–1360. <https://doi.org/10.1021/acs.jproteome.0c00129>